

## ELECTRONIC SUPPLEMENTARY INFORMATION

### Molecular spin qubits based on lanthanide ions encapsulated in cubic polyoxopalladates: Design criteria to enhance quantum coherence

José J. Baldoví,<sup>a,b</sup> Lorena E. Rosaleny,<sup>a</sup> Vasanth Ramachandran,<sup>c</sup> Jonathan Christian,<sup>c</sup> Naresh S. Dalal,<sup>c</sup> Juan M. Clemente-Juan,<sup>a</sup> Peng Yang,<sup>d</sup> Ulrich Kortz,<sup>d</sup> Alejandro Gaita-Ariño<sup>\*,a</sup> and Eugenio Coronado<sup>\*,a</sup>

<sup>a</sup> Instituto de Ciencia Molecular (ICMol), Universidad de Valencia, C/Catedrático José Beltrán 2, E-46980 Paterna, Spain.

<sup>b</sup> Institut de Chimie Moléculaire et des Matériaux d'Orsay, CNRS, Université de Paris Sud 11, 91405 Orsay Cedex, France.

<sup>c</sup> Department of Chemistry and Biochemistry, Florida State University, 32306 Tallahassee, FL (USA).

<sup>d</sup> Department of Life Sciences and Chemistry, Jacobs University, P.O. Box 750 561, 28725 Bremen (Germany).

**Table S11:** Crystal field splitting of TbPd12 calculated by the REC model assuming the Russell-Saunders coupling, REC model using the full hamiltonian and phenomenological fit of the  $\chi_m T$  product using the full hamiltonian.

	Tb (REC model)	Tb (REC CFPs in CONDON)	Tb (CONDON)
	0	0	0
	0	0	0
	0.1	1	2
	0.1	1	2
	0.1	1	2
	0.3	3	7
	220	172	158
	220	172	158
	220	172	158
	247	199	184
	247	199	184
	247	199	184
	283	235	217
B40	-1362	-1362	-1213
B60	503	503	411

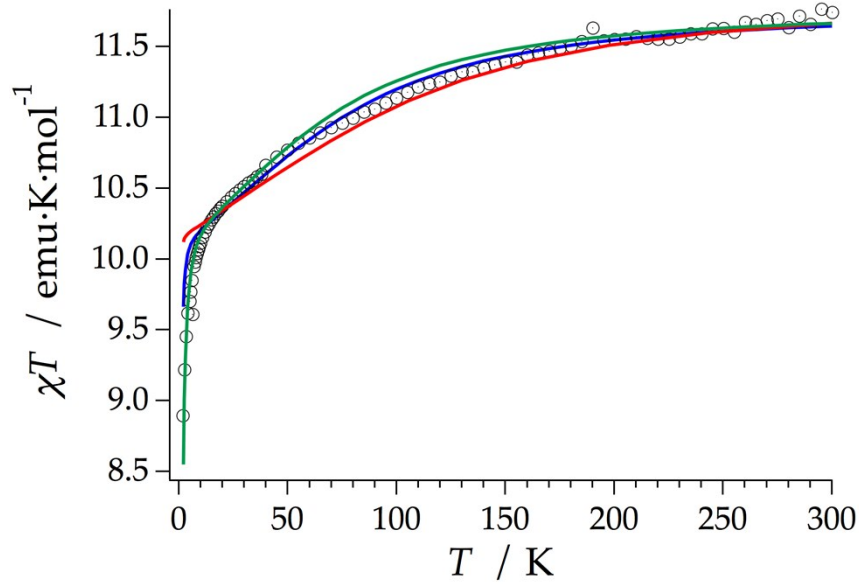


**Figure S11:** Comparison of the  $\chi_m T$  value of TbPd12 for powder from experiment (circles), REC model assuming Russell-Saunders scheme (red line), REC model using the full hamiltonian (blue line) and phenomenological fit using the full hamiltonian (green line).

**Table S12:** Crystal field splitting of DyPd12 calculated by the REC model assuming the Russell-Saunders coupling, REC model using the full hamiltonian and phenomenological fit of the  $\chi_m T$  product using the full hamiltonian.

	Dy (REC model)	Dy (REC CFPs in CONDON)	Dy (CONDON)
	0	0	0
	0	0.2	0.4
	0.8	0.4	4
	0.8	0.6	4
	0.8	7	4
	0.8	7	4
	68	57	56
	68	57	56
	68	57	56
	68	57	56
	288	278	251
	288	278	251
	347	328	304
	347	328	304
	347	328	304
	347	328	304
B40	-1260	-1260	-1127
B60	449	449	442

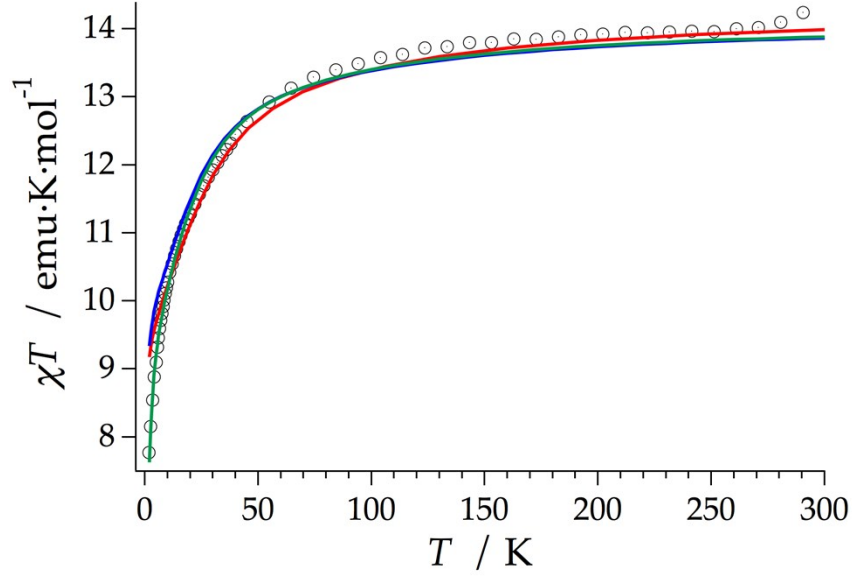


**Figure S12:** Comparison of the  $\chi_m T$  value of DyPd12 for powder from experiment (circles), REC model assuming Russell-Saunders scheme (red line), REC model using the full hamiltonian (blue line) and phenomenological fit using the full hamiltonian (green line).

**Table S13:** Crystal field splitting of HoPd12 calculated by the REC model assuming the Russell-Saunders coupling, REC model using the full hamiltonian and phenomenological fit of the  $\chi_m T$  product using the full hamiltonian.

	Ho (REC model)	Ho (REC CFPs in CONDON)	Ho (CONDON)
	0	0	0
	0	0	0
	2	0.9	2
	2	1	2
	2	1	2
	42	39	29
	42	39	29
	42	39	29
	311	280	260
	311	280	260
	325	294	276
	325	294	276
	325	294	276
	340	311	294
	382	347	314
	382	347	314
	382	347	314
B40	-1224	-1224	-1219
B60	428	428	384

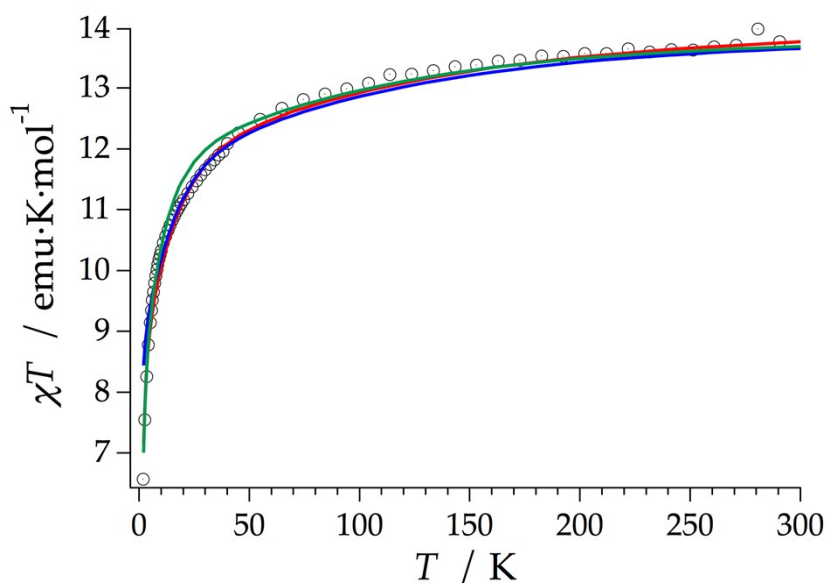


**Figure S13:** Comparison of the  $\chi_m T$  value of HoPd12 for powder from experiment (circles), REC model assuming Russell-Saunders scheme (red line), REC model using the full Hamiltonian (blue line) and phenomenological fit using the full Hamiltonian (green line).

**Table S14:** Crystal field splitting of ErPd12 calculated by the REC model assuming the Russell-Saunders coupling, REC model using the full Hamiltonian and phenomenological fit of the  $\chi_m T$  product using the full Hamiltonian.

	Er (REC model)	Er (REC CFPs in CONDON)	Er (CONDON)
	0	0	0
	0	0	0
	62	55	74
	62	55	74
	62	55	74
	62	55	74
	68	59	136
	68	59	136
	346	339	187
	346	339	187
	346	339	187
	346	339	187
	394	382	292
	394	382	292
	394	382	292
	394	382	292
B40	-1155	-1155	5
B60	391	391	288

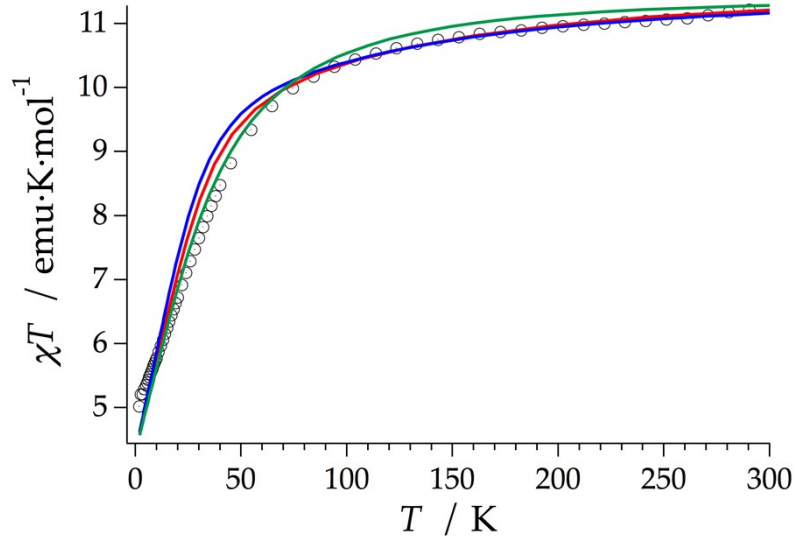


**Figure S14:** Comparison of the  $\chi_m T$  value of ErPd12 for powder from experiment (circles), REC model assuming Russell-Saunders scheme (red line), REC model using the full Hamiltonian (blue line) and phenomenological fit using the full Hamiltonian (green line).

**Table S15:** Crystal field splitting of TmPd12 calculated by the REC model assuming the Russell-Saunders coupling, REC model using the full Hamiltonian and phenomenological fit of the  $\chi_m T$  product using the full Hamiltonian.

Tm (REC model)	Tm (REC CFPs in CONDON)	Tm (CONDON)
0	0	0
91	86	116
91	86	116
91	86	116
156	151	246
156	151	252
391	383	252
391	383	252
391	383	286
424	417	286
426	424	421
426	424	421
426	424	421
B40	-1128	-1405
B60	375	510

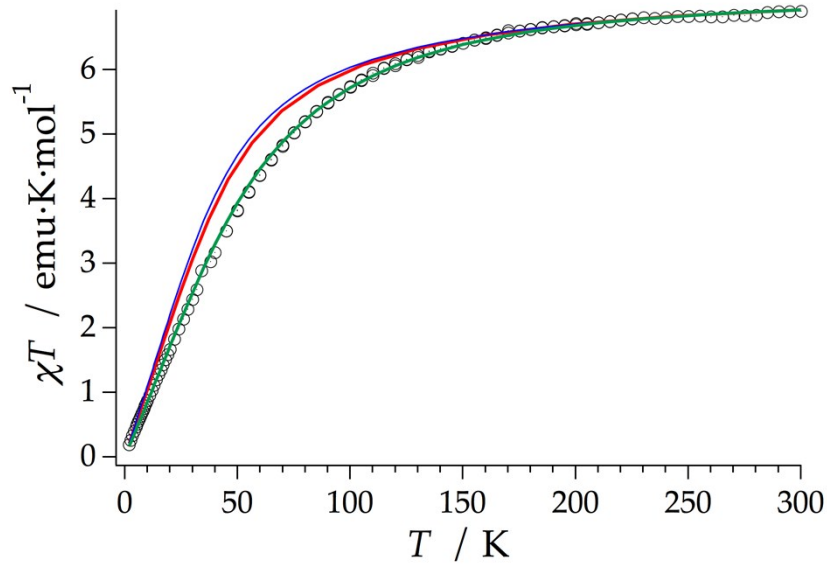


**Figure SI5:** Comparison of the  $\chi_m T$  value of TmPd12 for powder from experiment (circles), REC model assuming Russell-Saunders scheme (red line), REC model using the full Hamiltonian (blue line) and phenomenological fit using the full Hamiltonian (green line).

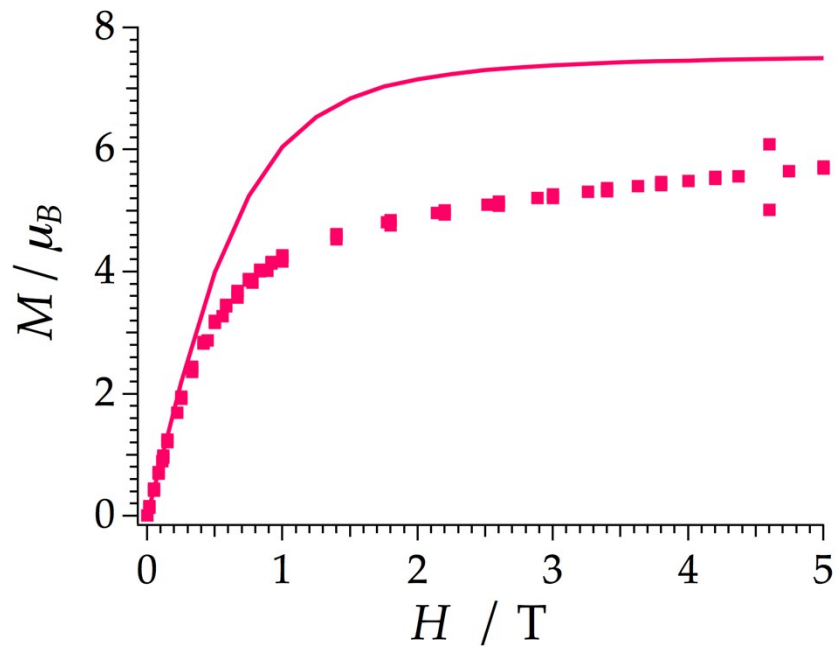


**Figure SI6:** Experimental (markers) and calculated with the REC model in the SIMPRE package (solid line) magnetization of TbPd12 at 2 K with an applied magnetic field varying between 0 and 5 T.

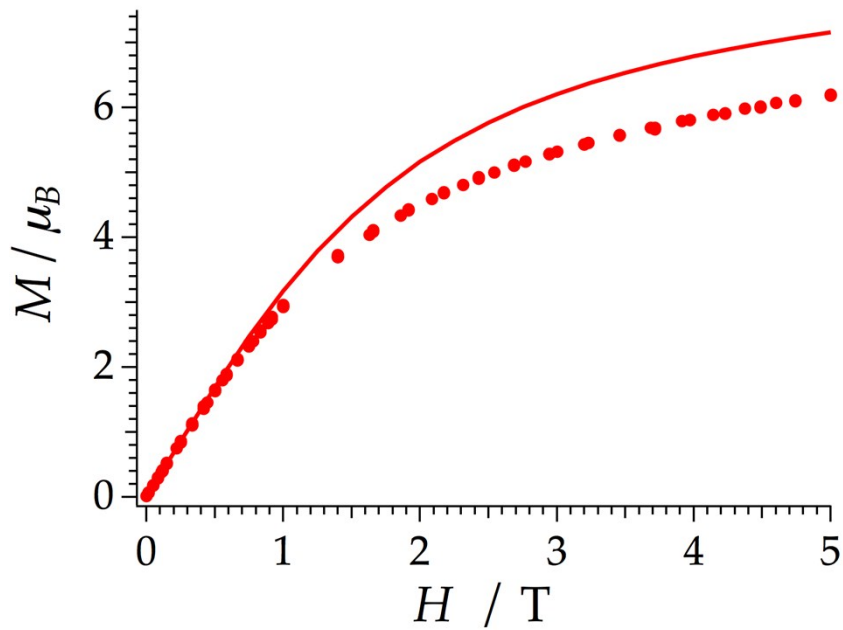


**Figure SI7:** Experimental (markers) and calculated with the REC model in the SIMPRE package (solid line) magnetization of DyPd12 at 5 K with an applied magnetic field varying between 0 and 5 T.

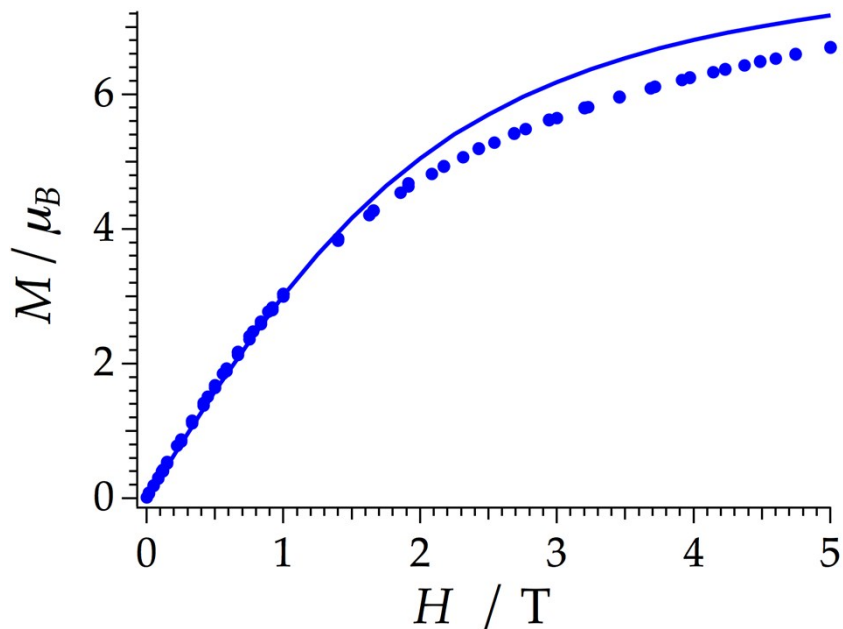


**Figure SI8:** Experimental (markers) and calculated with the REC model in the SIMPRE package (solid line) magnetization of HoPd12 at 5 K with an applied magnetic field varying between 0 and 5 T.

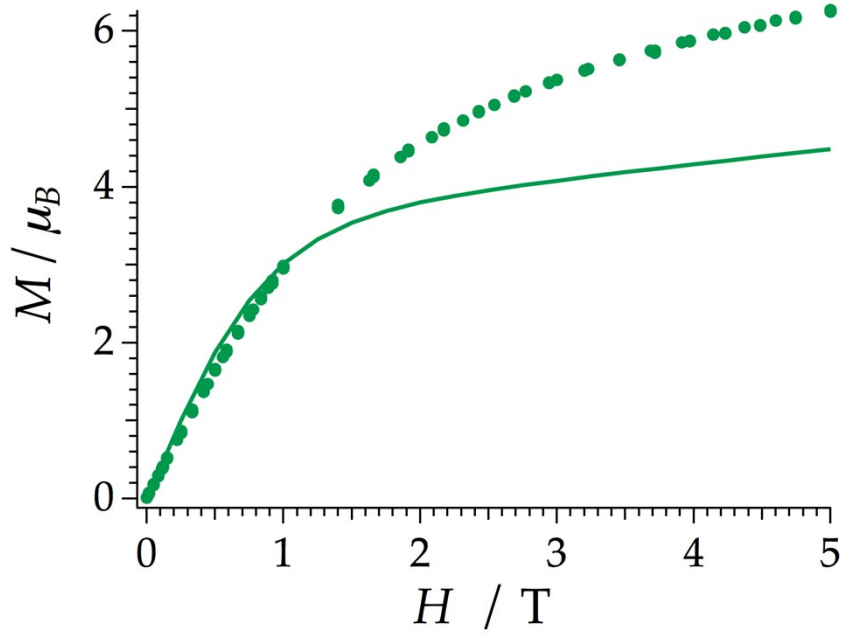


**Figure S19:** Experimental (markers) and calculated with the REC model in the SIMPRE package (solid line) magnetization of ErPd12 at 2 K with an applied magnetic field varying between 0 and 5 T.

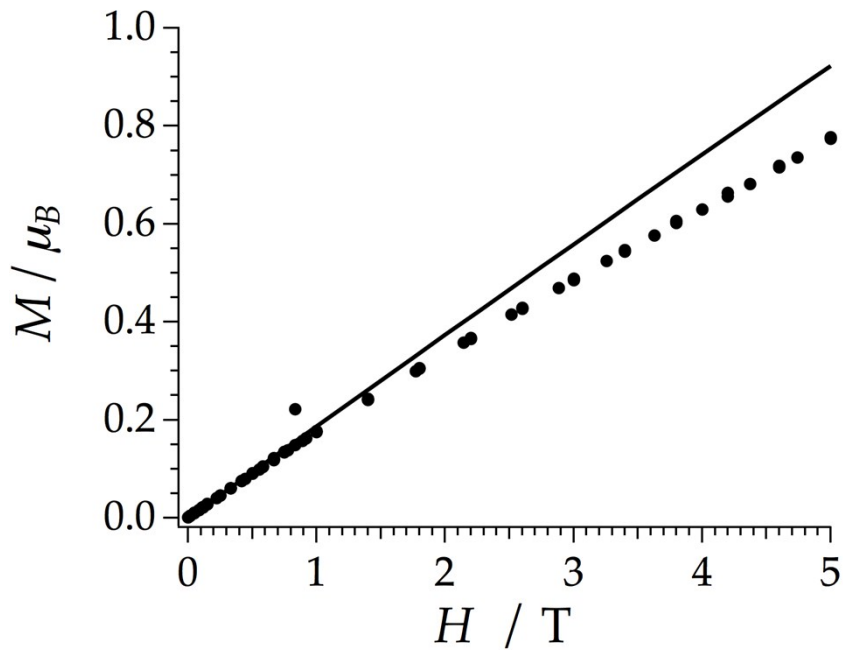


**Figure S110:** Experimental (markers) and calculated with the REC model in the SIMPRE package (solid line) magnetization of TmPd12 at 1.8 K with an applied magnetic field varying between 0 and 5 T.



## Methodology: calculation of the decoherence times

We follow the methodology reported in Ref. 1.<sup>1</sup> The crystal field Hamiltonian was solved with SIMPRE. A minor modification allows introducing the magnetic field as a diagonal component in the Hamiltonian. From the energy level structure in the presence of this field, it is immediate to obtain  $\Delta$  as the energy differences between the ground state and the first excited state.

SIMPRES was further adapted to extract the expectation values of  $\langle J_\alpha \rangle$  (with  $\alpha=x,y,z$ ) from the wave functions, using the Pauli matrices  $\sigma_\alpha$ .

Moreover, this specially crafted version of SIMPRE also takes the coordinates of the hydrogen atoms as input. Of course, there is an effectively infinite number of hydrogen nuclei in a crystal structure. A cutoff radius for the hydrogen nuclei to be included in our calculation is needed. We neglect every hydrogen nucleus, which on average, is expected to produce 1/100<sup>th</sup> of the effect produced by the hydrogen nucleus closest to the metal. As the hyperfine interaction falls with the third power of the distance, this means the cutoff radius is a factor of (100)<sup>1/3</sup> farther away than the nearest hydrogen atom.

From the expectation values of  $\langle J_x \rangle, \langle J_y \rangle, \langle J_z \rangle$  and these coordinates, the dipolar magnetic field (H) felt by each nucleus and the hyperfine interaction energy (E) can be trivially calculated, for each of the two states of the qubit.

From the set of hyperfine interactions, we estimate the nuclear spin bath decoherence time using standard equations.<sup>2</sup> This estimate of decoherence depends on the sum of the energy differences, for each proton  $i$  between the two qubit states  $|0\rangle, |1\rangle$ . The decoherence time is then estimated as a function of the tunneling gap  $\Delta$  and this energy sum ( $\omega_i = E_0 - E_1$ );  $\tau = \Delta / ((\sum \omega_i)^2)$ .

### Wave functions, expected values of $J_z$ for ground and excited states, and $\tau_n$ at two different field/compressions

- **0.85% compression and an applied field of 0.35 T**

$$|\psi_0\rangle = 20\%|-8\rangle + 68\%|-4\rangle + 9\%|+4\rangle + 2.4\%|+8\rangle$$

$$|\psi_1\rangle = 2.6\%|-8\rangle + 8.7\%|-4\rangle + 68.7\%|+4\rangle + 20\%|+8\rangle$$

$$\langle J_{z0} \rangle = -3.78$$

$$\langle J_{z1} \rangle = 3.76$$

$$\tau_n = 1.84 \cdot 10^{-3} \text{ s}$$

- **0.78% compression and an applied field of 0.39 T**

$$|\psi_0\rangle = 20\%|-8\rangle + 69.7\%|-4\rangle + 7.4\%|+4\rangle + 2\%|+8\rangle$$

$$|\psi_1\rangle = 28.2\%|-6\rangle + 24.4\%|-2\rangle + 22\%|+2\rangle + 24.2\%|+6\rangle$$

$$\langle J_{z0} \rangle = -3.94$$

$$\langle J_{z1} \rangle = 0.33$$

$$\tau_n = 7.48 \cdot 10^{-3} \text{ s}$$

---

<sup>1</sup> L.E. Rosaleny, A. Gaita-Ariño, *Inorg. Chem. Front.*, 2015, submitted.

<sup>2</sup> S. Takahashi, I.S. Tupitsyn, J. van Tol, C.C. Beedle, D.N. Hendrickson and P.C.E. Stamp, *Nature*, 2011, **476**, 76-79.